ABCM 40 anos — Associação Brasileira de Engenharia e Ciências Mecânicas

CONEM 2016
CONGRESSO NACIONAL DE ENGENHARIA MECÂNICA

21 - 25 AGOSTO DE 2016
FORTALEZA - CEARÁ

Unsteady Flow Field in a Shock Tube: Solutions, CFD and Experiments

Bruno Coelho Lima, brunocoelho@ ieav.cta.br[1]
Jayme Rodrigues Teixeira da Silva, jaymerts@ieav.cta.br[1]
João Felipe de Araújo Martos, joaomartos@gmail.com[1]
Paulo Gilberto de Paula Toro, toro@ieav.cta.br[2]
Marco Antônio Sala Minucci, sala@ieav.cta.br[2]
Antônio Carlos de Oliveira, acoc@ieav.cta.br[2]
Álvaro Francisco Santos Pivetta, pivetta@ ieav.cta.br[1]
Ana Maria Pereira Lara, anamariapereiralara@gmail.com[1]
Israel da Silveira Rego, israel.rego@ieav.cta.br[2]

[1] Instituto Tecnológico de Aeronáutica (ITA), Praça Marechal Eduardo Gomes, n° 50, Vila das Acácias, CEP 12228-900, São José dos Campos/SP-Brasil.
[2] Instituto de Estudos Avançados (IEAv), Trevo Coronel Aviador José Alberto Albano do Amarante, n° 1, Putim, CEP 12.228-001, São José dos Campos/SP-Brasil.

Abstract: *The shock tube is a ground-facility widely used in aerospace and aeronautics science and technology for studies on gas dynamic and chemical-physical processes in gases at high-temperature, explosions anddynamic calibration of pressure sensors. A shock tube consists ofa long cylindrical tube with same cross-section, which is separated by a thin membrane, called diaphragm, into two parts. One of them, the low-pressure tube or driven, is filled with the test gas, while the compressed gas is fed into the second part or driver. Ideally, when the diaphragm is suddenly bursted, the compressed driver gas flows into the driven tube, forming instantly a moving shock wave that propagatesthrough the test gas. The distribution of the various physical properties through the shock front is represented as "jumps". After the shock front reaches the shock tube end, it is reflected towards the driver tube, increasing sharply the physical variables over the values behind the incident shock. The aim of this paper is to investigate the transient flowfield and phenomena in a shock tube by means of gas-dynamic theory, computational fluid dynamics (CFD) simulations and shock tube experiments. First, solutions for ideal shock tube operation are calculated, followed by inviscid and viscous CFD simulations. Finally, gas-dynamic experiments in T1 shock tube of IEAv are carried out. Preliminary CFD verification and validation of unsteady shock tube airflow are the following: Inviscid and viscous CFD simulations are in good accordance with ideal shock tube solutions for weak shocks, indicating that the computer programming errors are low (less than 5 %); and both CFD simulations overestimate the experimental results, showing that the sudden diaphragm rupture still need to be considered. Experience and lessons learned herein can be considered with confidence for decision making in shock tube design.*

Palavras-chave: *shock tube, moving shock wave, transient simulation*

1. INTRODUÇÃO

It has always been fundamental to validate any research laboratory tests, and shock tubes are excellent device. Reliable, versatile, and relatively low cost mainly for the aerospace sector a test flight can expend millions of dollars. Even with the advent of shock tunnels that can reach higher speeds, the shock tubes are laboratory facility widely used despite having reduced test time (order of microseconds), are able to simulate conditions with gases at high pressures and temperatures and therefore high enthalpy. According to Lukasiewicz (1952) and Glass and Hall (1959) shock tube was first used by Vielle in France in 1899 to study flame's problem. This capability makes an efficient ground test tool used "in various fields such chemistry, physics, fluid dynamics, structures and astrophysics" (Mantovani et al, 2011).

Several work on shock tubes have already been presented, however it is difficult to find papers that present simulations, analytical and experimental. Simulations numerological viscous (CFD) should be used more frequently to make it possible to see the physical phenomena impossible to detect in a shock tube, for example: boundary layer, shock wave iteration with the surface of contact, detachment of the boundary layer and others.

Nowadays we have several tools to assist in the shock tube design, can estimate the losses and increase efficiency. Perhaps CFD simulations are the most powerful tools, however simulate flow at high speeds is still a hard task always requiring experimental validations.

This paper hopes to show the behavior of aerothermodynamics properties of a shock tube while it is in valid test of time, that is, while the wave reflected shock not find the contact surface. It will be made comparison among analytical calculations, simulations and experiments, was used the shock tunnel T1 of IEAv to conduct experiments and dimensions for the simulations. For analytical data will use the ideal exact solutions in Python in house routine, simulations CFD (computer fluid dynamic) ANSYS FLUENT solver, and for the experiments was used data from experiments carried out in Prof. Henry T. Nagamatsu Laboratory of Aerothermodynamics and Hypersonic that used the shock tube T1.

2. Methodology

2.1. Operation of a shock tube

A shock tube in its simplest form is comprised of two separate tubes of equal cross-section by a diaphragm. The diaphragm function is to separate the two reservoirs at different pressures. The reservoir containing high pressure is called the Driver, the gas will initially be home is get the index (4). The gas at low pressure at rest also receive the index (1) and its respective reservoir is called driven "Fig. 1 "

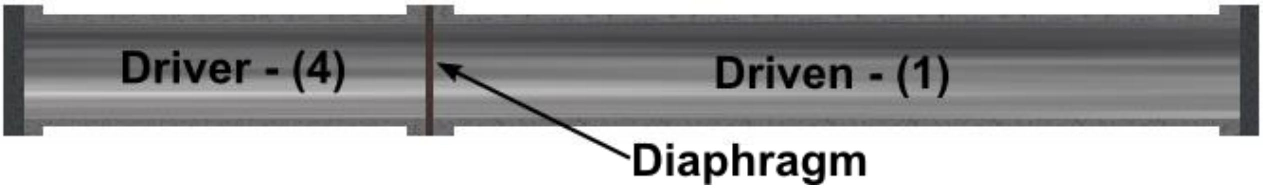

Figure 1: Simplified scheme of a shock tube

The shock tube operation begins when the two reservoirs are pressurized, for this work we consider an ideal case: adiabatic, reversible pressurization, gas behaving as ideal gases, suddenly break the diaphragm and neglecting the forces viscous.

When the diaphragm are broken ideally by pressure difference, a normal shock wave and non-stationary will be formed in the same place of diaphragm and will get around toward the closed end of Driven with U_s speed, this shock wave are named incident shock wave. Simultaneously a series of wave of expansion will be formed and move towards the end of the driver, the front of this expansion wave moves around with a_4 speed (Speed of sound driver gas).

The gas resting on Driven will feel the passage of the shock wave heated to a temperature T_2, compressed to a pressure P_2 and accelerated up to a speed U_2 an irreversible process S_2. Similarly the gas in the driver (also at rest) will be cooled to a temperature T_3, expanded to a pressure P_3, (which is equal to P_2) and accelerated up to a U_3 speed (which is equal to U_2) in a reversible process S_3 . Due to the short time and the large gradient of the properties, the gases they felt the passage of the wave incident shock and the series of expansion waves will not interact. Thus forming a impermeable membrane called the contact surface, which will walk the a_2 speed towards the end of Driven “Fig. 2”

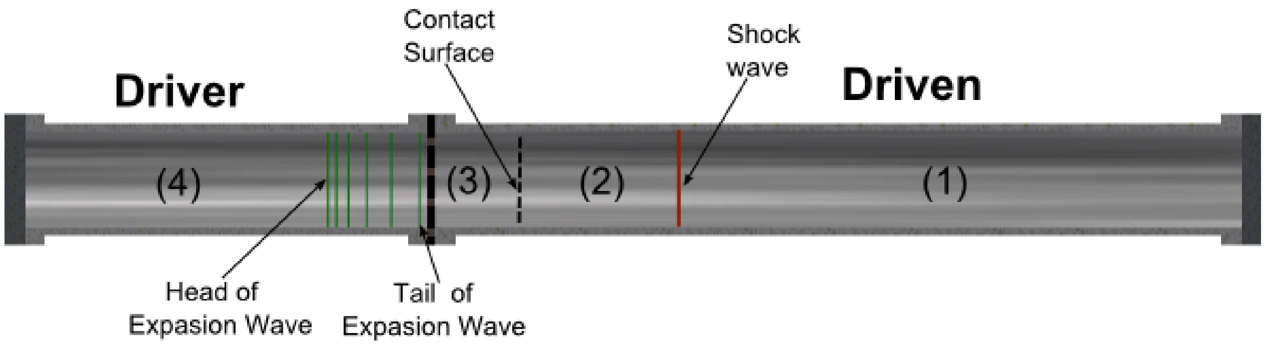

Figure 2: Physical Phenomena in a Shock Tube

For aerodynamics tests in shock tube the gas behind of shock wave is one have velocity and constant properties necessary for an aerodynamic study. This gas is found in a shock tube until the incident shock wave reflected reach the driver end, reflect and interact with the contact surface. After fully reflect the end of the driver, the incident shock wave will be called reflected shock wave and indicated with index (r) “Fig. 3”. The reflected shock wave, will accelerate the gas at same velocity however opposite direction $(u_5 = 0)$.

Now the gas before accelerated by the wave incident shock, return to the rest. The gas that sense the passage of the reflected shock wave is abruptly stagnant and receive the index (5), this gas will be compressed to a pressure P_5, at a temperature T_5, an irreversible process S_5. Normally this gas is in the high enthalpy due to high temperature, and used for the study of combustion, chemical kinetics, and others. It is useless to the aerodynamic study due to lack of speed. Likewise, the front wave of expansion to find the end of the Driver will completely reflect, and change its direction, moving now to the end of Driven.

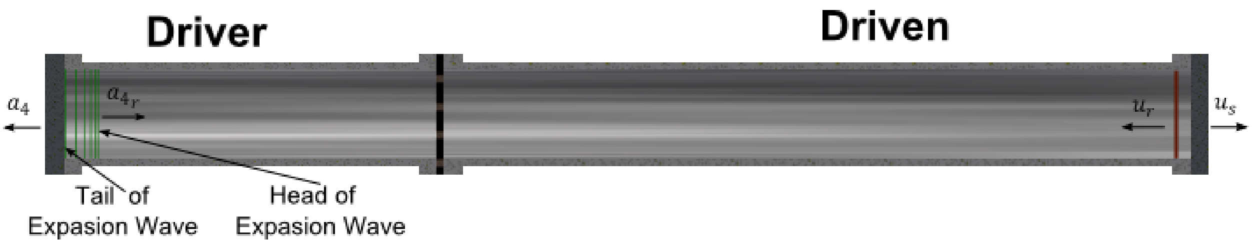

Figure 3 - Incident Shock Wave and Front of Expansion Wave Reflecting

To describe the flow in a shock tube is used 4 equations known as Navier-Stokes equations. These equations demonstrate the principles of conservation in a thermodynamic system, and adds the principle of entropy for non-isentropic flow like the case of a normal shock wave. The equations are:

- Continuity Equation :
- Momentum Equation
- Energy Equation
- Second law of Thermodynamics.

2.2. Exact Solution

Manipulating the above equations and considering the one-dimensional flow, gas behave as ideal gas, adiabatic, burst diaphragm disruption is possible arrives in the exact solution for shock tubes. All equations for the exact solution can be obtained in Anderson (2011), Ferri (1961) e Nagamatzu (1958). In this paper as we pay attention only to the distribution of pressure, because it was the thermodynamic property withdrawal of experiments. The ratio of pressure across of shock wave (where γ is the ratio of specifics heats):

$$\frac{p_2}{p_1} = \frac{2\gamma_1 M_s^2 - (\gamma_1 - 1)}{\gamma_1 + 1} \tag{1}$$

Considering the expansion due to series wave expansion is isentropic (Ferri 1961, Nagamatzu, 1958) we find the shock tube relation. This relationship by mathematical iteration allows finding the power of the incident shock wave, in other words how high is your Mach number. "Fig. 4" show the behavior of this equation.

$$\frac{p_4}{p_1} = \frac{p_2}{p_1}\left\{1 - \left[\frac{a_1(\gamma_4 - 1)}{a_4(\gamma_1 + 1)}\right]\left(\frac{M_s^2 - 1}{M_s}\right)\right\}^{-\frac{2\gamma_4}{(\gamma_4 - 1)}} \tag{2}$$

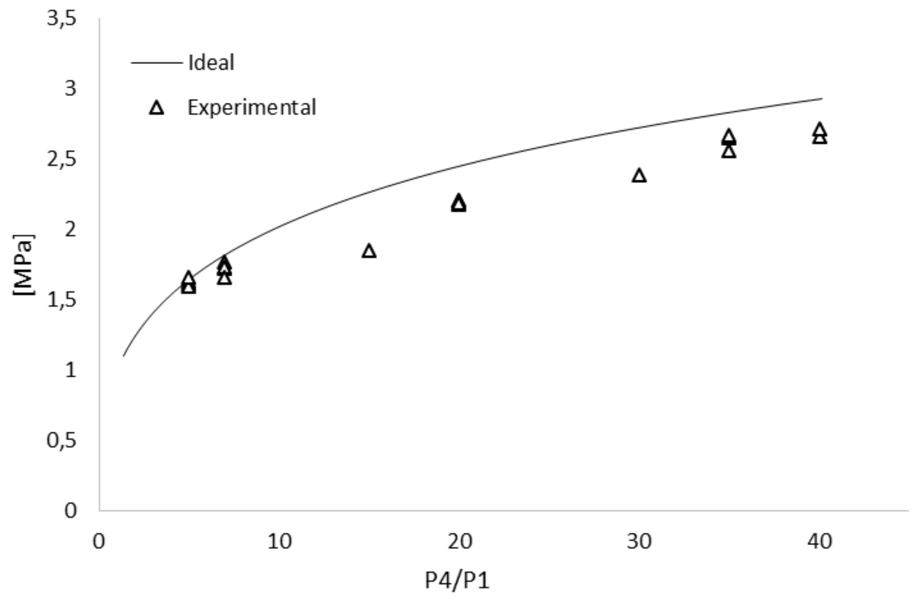

Figure 4 – Behavior of Ms as function by P4/P1

The Mach number of the reflected shock wave can be rewritten as a function of Mach number of the flow behind the incident shock wave. The Mach number of the reflected shock wave can be writer by function of Mach number of the incident shock wave:

$$\frac{M_r}{M_r^2-1}=\frac{M_s}{M_s^2-1}\sqrt{1+\frac{2(\gamma_1-1)}{\gamma_1+1}\left(M_s^2-1\right)\left((\gamma_1+1)\frac{1}{M_s^2}\right)} \quad (3)$$

Analogously to the modeling of the flow and using same concepts, known properties after the incident shock wave is possible determinate the conditions after passing of reflected shock wave.

$$\frac{p_5}{p_2}=\frac{2\gamma_1 M_r^2-(\gamma_1-1)}{\gamma_1+1} \quad (4)$$

2.3. Simulações Numéricas

For numerical analysis Ansys's solver Fluent was used in transient state, with the Implicit Roe's Averaged Method (Roe, 1981), second order in space and first order in time, by finite volume method. Because of computational limits, some simplifications were necessary where the largest of them were considering that the diaphragm is instantly retired and no real gas model is used because the operation conditions are close to 1000k.

This task was broken into three stages, in the first step the flow is considered to be one-dimensional and discards the viscous forces, this way we can conclude that $\frac{\partial_y}{\partial_t}=0$, which enables the use of an one-dimensional mesh "Fig. 5", because there is no viscosity influence, the tank's length is overlooked as its circular shape.

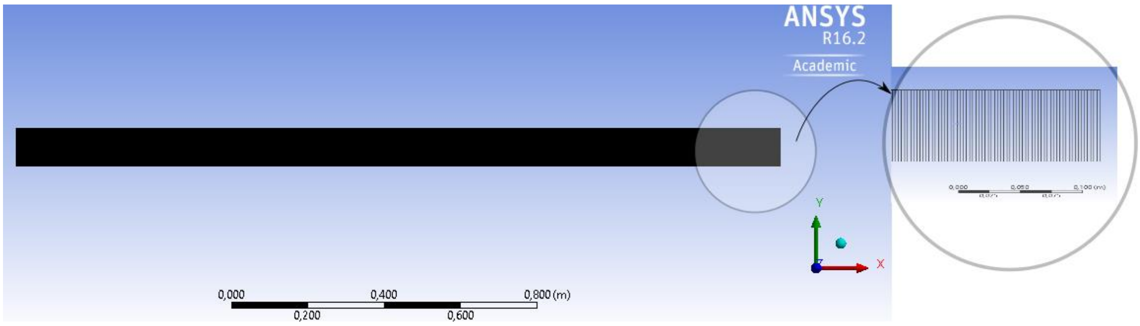

Figure 5 – Unstructured Mesh

Before executing the computational analysis, bibliographic research and ideal case's validation were performed by comparing with Al-Falahi, at all, (2010) e Ksibi,H. et al (2008) works. Only after that, numerical analysis was started. Mesh convergence was reached by reducing the element size up to variations of the control volume physical property less than 2%. Also, the residuals were kept low than 1E-6 in every time step. It is clear that after an element's quantity, there is no more thermodynamic properties influence of results, only graphic contour difference. That is, increasing elements number we move towards a non-smoothing pressure, temperature, density etc. gradients, producing well featured plateaus. Simulations were performed for pressure ratios across the diaphragm of: 10, 20, 30, 40 and 50.

The second stage of this study considers the viscous forces effect with laminar flow. In this case cannot be used the same mesh (one-dimensional) because $\frac{\partial_y}{\partial_t} \neq 0$. The geometry was reproduced from a circular revolution's section (axisymmetric), close to the wall the mesh was refined in order of make the thermodynamic properties convergence easiest on the boundary layer region "Fig. 5".

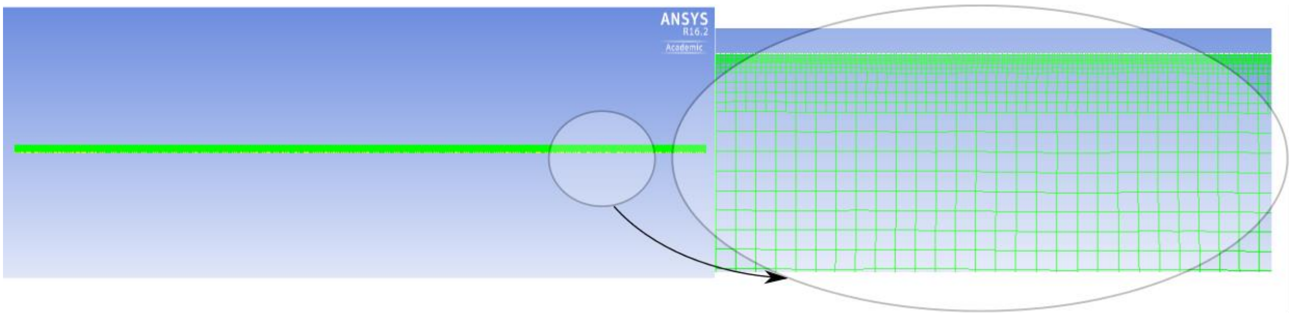

Figure 6 – Mesh for viscous case

At the third stage turbulence effects are include ($k - \varepsilon$), Lamnaouer (LAMNAOUER, 2004) says that should not see difference between the turbulent and laminar calculation values, or between turbulence models available in the software (there is no difference in property values when turbulence models are changed, only the contours variations). It happens because the flow is laminar until the gas behind of the reflected shock wave interact with flow behind the contact surface, what means the end of analysis, because the flow will not remain constant thermodynamic conditions. The third stage results were not presented because the second and third section's variation was too small, a little comparing are show in "Table. 1".

Table 1. Laminar and turbulent simulations comparison for pressure ratio of 50 atm across the diaphragm.

Found Pressures	Laminar	$k - \varepsilon$ Standart	$k - \varepsilon$ RNG
P5 (Mpa)	56,57	55,24	54,99
P2 (Mpa)	11,11	11,05	10,95

2.4. Experiment

The preparation of the experiment consists in positioning the diaphragms increase the pressure of high-pressure reservoir (Driver) gradually to avoid heating of gas making more isentropic pressurization possible as it can. Knowing that a shock tube test time is extremely small, must be used sensors and data acquisition system compatible with this time, for example, piezoelectric sensors. The sensors must be installed at the end of the low-pressure reservoir, because in this region the flow felt all effects of viscosity and losses all the energy, which will be exposed during the test

"Fig.7". Knowing the distance of sensors and the time spend of shock wave for crossing this distance, is determined the speed of Shock Wave.

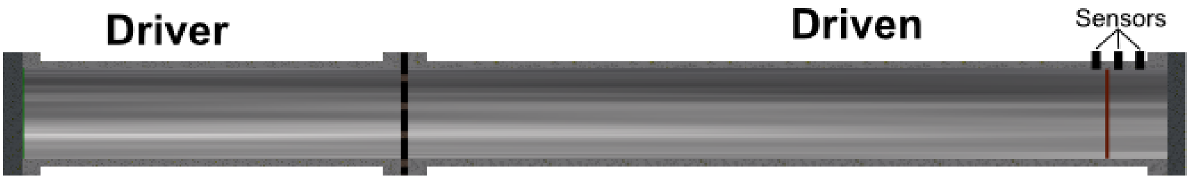

Figure 7 – Operating diagram of a shock tube with sensors installed at the end of Driven

All sensors were connected to an oscilloscope, but not directly, someone models require signal conditioning and other needs amplifiers. Knowing the sensitivity of the sensors and the signals voltages of oscilloscopes is possible calculate the pressure measured by each sensor. The experimental data of this paper were taken from internal research realized in the Laboratory of Aerothermodynamics Hypersonic at IEAv in shock tube T1.

3. Results

Validation of ideal simulations (neglecting viscous forces) was performed with the analytical calculations, the accuracies of the simulations were excellent, the errors of all properties (or ratios) were below 2%. In "Figure 8" can see the pressure ratio across the shock wave incident in function of the ratio through the diaphragm; this shows the power of the Shock Wave.

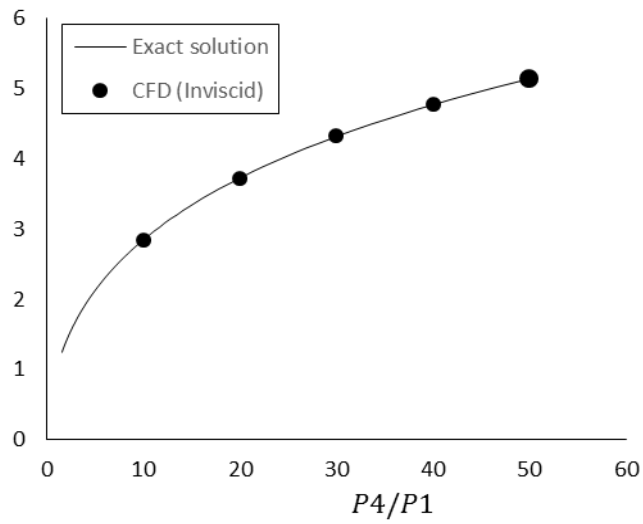

FIGURA 8 – Comparison between simulation (CFD) and analytical both inviscid

Comparing ideal simulations with the viscous (laminar) "Fig. 9", it is possible to see that error decreases as the increases speed of the incident shock wave. This is expected because the viscous forces are only prevalent in the flow at low speeds, when it is greater than the forces of inertia present in the gases.

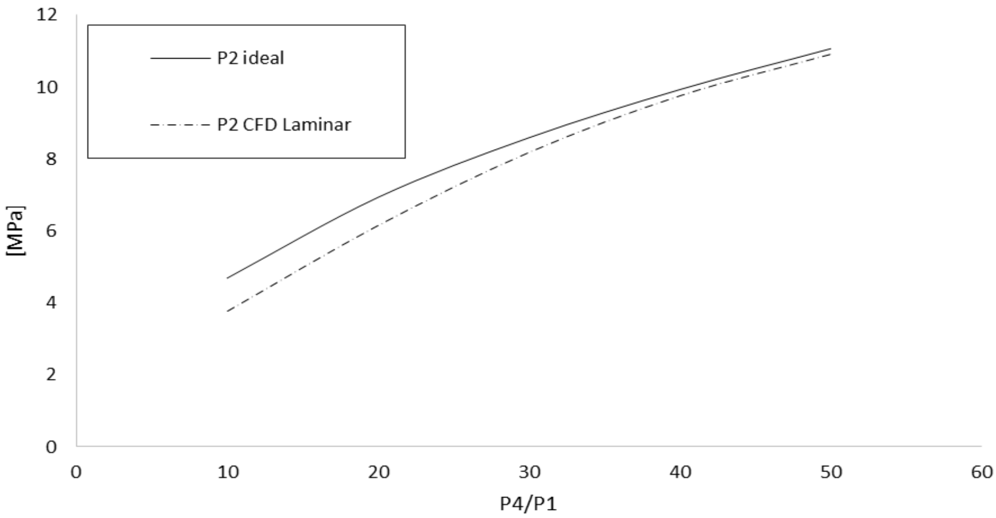

Figura 9 – Comparison between simulations (CFD) Viscous, inviscid and experimental for a shock tube

Comparing the simulation with experimental cases “Fig. 10”, can see the error of the analytical calculation and simulations increases as the pressure ratio across the diaphragm increases and consequently the speed of the incident shock wave increases. This error should be caused by not instantaneous diaphragm opening, which were not considered in the simulations because of lack of a computational power.

When the pressure ratio of reservoir increases, the thickness of diaphragm needs increases too, requiring more energy to break it. The opening time is also slower due to the increased thickness, causing more losses, the opening time of the diaphragm cause a delay on the formation of the shock wave, and it occurs approximately 10 times the diameter of the tube Driven. This delay in the opening decreases the strength of the shock wave, resulting in an increasingly significant loss of pressure.

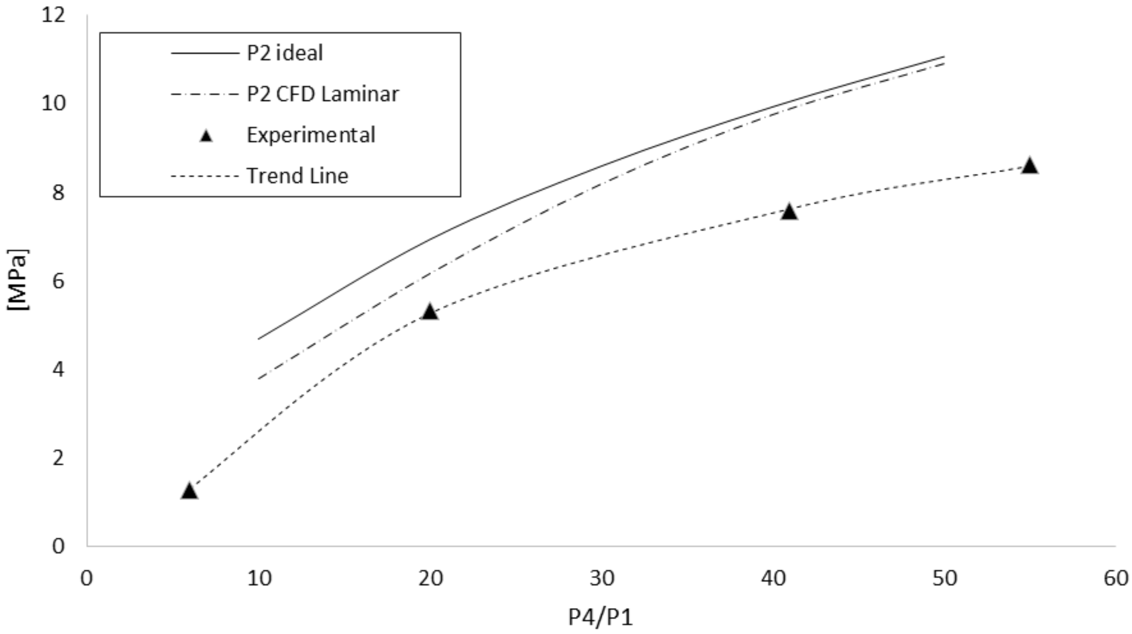

Figure 10 - Physical validation of simulations (CFD) of the pressure behind the incident shock wave, comparison between simulations and experiments

The same phenomenon occurs when we compare the simulations with the values obtained by experimental means "Fig. 11". The loss caused by the aperture of the diaphragm increases when the pressures across the diaphragm higher and the losses by viscous forces are becoming smaller

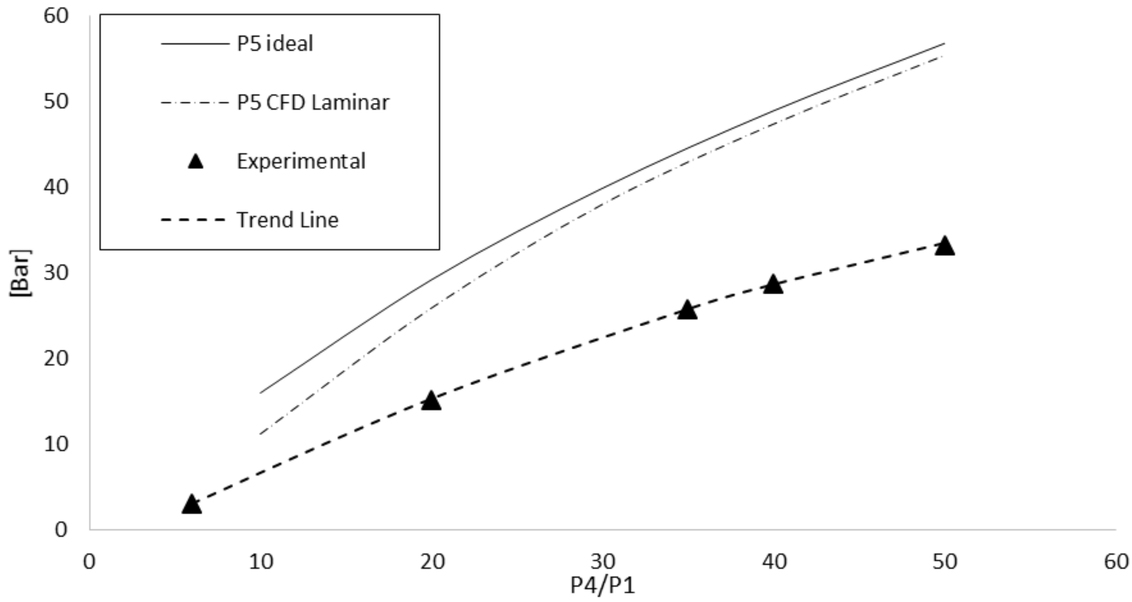

Figure 11. Physical validation of simulations (CFD) of the pressure behind the reflected shock wave, comparison between simulations and experiments

Besides serving as results of comparison tool, CFD can help understanding the operation of a shock tube. As the fluid behavior over driven "Fig. 12" and others phenomena that impossible to see during the experiment. If added turbulence models it is possible see the interaction between the reflected shock wave and the boundary layer (the pressure gradient causing the detachment of the boundary layer) and the flow behavior when the flows behind the contact surface (condition 3) interact with gas stagnant by the reflected shock wave.

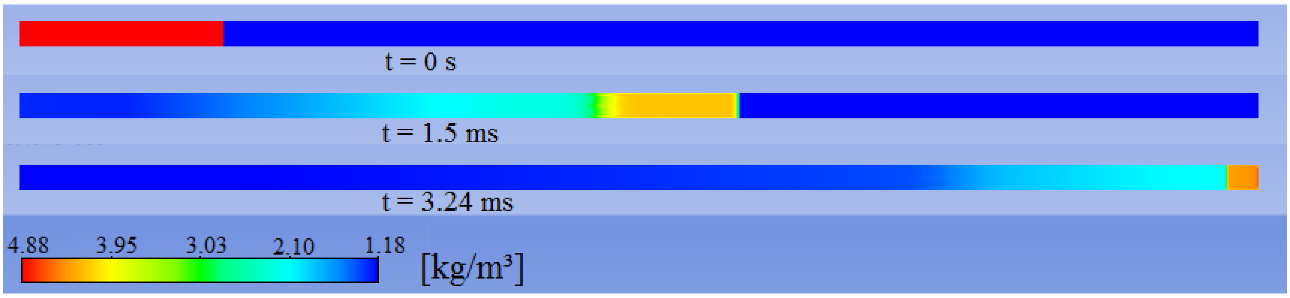

Figure 12. Shock Tube operation in different time step shown by the contorn density: initial, incident shock wave moving along driven and reflected shock wave going to Driver's end.

4. Conclusion

It may be noted in the experimental data "FIG. 10" and "Fig. 11" the same behavior a decreasing pressure as that speed increases, the tendency curve of the experimental data in both cases followed a pattern, a second degree equation. This loss are caused by various reasons such as viscous forces, pressurization not isentropic, diaphragm rupture and others. It was noted that the viscous forces are weaker and weaker as the speed of the incident shock wave (consequently the reflected shock wave) increases.

The viscous simulations (CFD) gave a great help because analytical calculations involving a shock tube are not trivial and not allow to "see" what happens in the flow.

The main contributions of this paper were to prove that viscous forces lose power over the flow to as your speed increases and give dimension of the influence that aperture impose at flow. This study may in some way assist in new designs of shock tubes, as well as helping to understand the behavior of aerothermodynamics properties of a shock tube in real cases and helping to stipulate real conditions experiments.

5. REFERÊNCIAS (Times New Roman, negrito, tamanho 10)

Ferri, A. 1961, "Fundamental Data Obtained from Shock Tube Experiments", chapter III, "Shock Tube Technology and Design" (Nagamatsu, H. T.), Pergamon Press, 1961.

Mantovani, A. F., Romanelli Pinto D., Toro, P. G. P., Minucci, M. A. S., 2011, "Shock Tube Operation, Flow Modeling and Theoretical Analysis", 21st Brazilian Congress of Mechanical Engineering. October 24-28, 2011, Natal, RN, Brazil.

Roe, P.L.,1981, "Approximate Riemann Solvers, Parameter Vectors, and Difference Schemes" , Journal Of Computational Physics, 43, pp 357-372.

Lukasiewicz, J., 1952, "Shock Tube Theory and Applications". National Aeronautical Establishment, Rept. 15, Otawwa, Canada.

Nagamatsu, H. T., 1958, "Shock Tube Technology and Design", Report No. 58-RL-2107, General Electric Research Laboratory, Schenectady, New York.

Anderson JR., J. A., 2011, "Fundamental of Aerodynamics" McGraw-Hill, Inc., 5th edition.

Lamnaouer, mouna, 2004, Numerical Modeling Of The Shock Tube Flow Fields Before And During Ignition Delay Time Experiments At Practical Conditions, Ph.D. thesis, Florida, United States of America.

Al-Falahi Amir, Yusoff M. Z, Yusaf T , 2010, "Numerical Simulation of Inviscid Transient Flows in Shock Tube and its Validations", International Journal of Mathematical, Physical and Engineering Sciences 4:1.

Ksibi. H, Moussa, A. B., 2008, "Numerical simulation of a one-dimensional shock tube problem at supercritical fluid conditions", International Journal of Physical Sciences Vol. 3 (12), pp. 314-320.

Glass, I.I. and Hall, J.G., 1959, Shock Tubes". Handbook of Supersonic Aerodynamics, section 18. Navord Report 1488 (vol. 6).

6. COPYRIGHT LIABILITY

"The authors are the only responsible for the content of this work."